Available online at www.sciencedirect.com

SciVerse ScienceDirect

Nuclear Physics B 873 (2013) 275–292

NUCLEAR PHYSICS B

www.elsevier.com/locate/nuclphysb

Measurement of the effective $B_s^0 \to J/\psi K_S^0$ lifetime ☆

LHCb Collaboration

Received 17 April 2013; accepted 25 April 2013

Available online 29 April 2013

Abstract

This paper reports the first measurement of the effective $B_s^0 \to J/\psi K_S^0$ lifetime and an updated measurement of its time-integrated branching fraction. Both measurements are performed with a data sample, corresponding to an integrated luminosity of 1.0 fb^{-1} of pp collisions, recorded by the LHCb experiment in 2011 at a centre-of-mass energy of 7 TeV. The results are: $\tau^{\text{eff}}_{J/\psi K_S^0} = 1.75 \pm 0.12$ (stat) ± 0.07 (syst) ps and $\mathcal{B}(B_s^0 \to J/\psi K_S^0) = (1.97 \pm 0.23) \times 10^{-5}$. For the latter measurement, the uncertainty includes both statistical and systematic sources.

1. Introduction

In the Standard Model (SM), CP violation arises through a single phase in the CKM quark mixing matrix [1]. In decays of neutral B mesons (B stands for a B^0 or B_s^0 meson) to a final state accessible to both B and $\overline{B}$, the interference between the amplitude for the direct decay and the amplitude for decay via oscillation leads to time-dependent CP violation. A measurement of the time-dependent CP asymmetry in the $B^0 \to J/\psi K_S^0$ mode allows for a determination of the B^0–$\overline{B}^0$ mixing phase ϕ_d. In the SM it is equal to 2β [2], where β is one of the angles of the unitarity triangle in the quark mixing matrix. This phase has already been well measured by the B factories [3,4], but further improvements are still necessary to conclusively resolve possible small tensions with the other measurements constraining the unitarity triangle [5]. The latest average composed by the Heavy Flavour Averaging Group (HFAG) is $\sin\phi_d = 0.682 \pm 0.019$ [6]. To achieve precision below the percent level, knowledge of the doubly Cabibbo-suppressed higher order perturbative corrections, originating from penguin topologies, becomes mandatory. These contributions are difficult to calculate reliably and therefore need to be determined directly from experimentally accessible observables.

☆ © CERN for the benefit of the LHCb Collaboration.

0550-3213/
http://dx.doi.org/10.1016/j.nuclphysb.2013.04.021

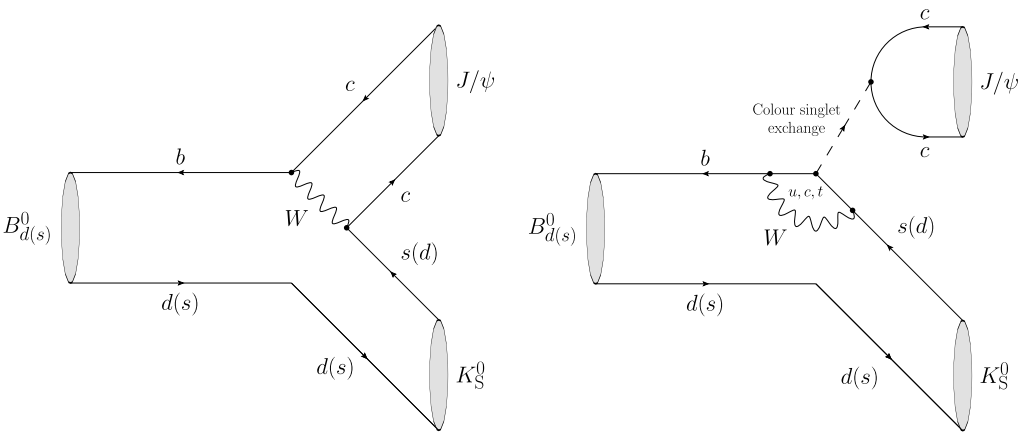

Fig. 1. Decay topologies contributing to the $B_{d(s)} \to J/\psi K^0_S$ channel: (left) tree diagram and (right) penguin diagram.

From a theoretical perspective, the $B^0_s \to J/\psi K^0_S$ mode is the most promising candidate for this task. It is related to the $B^0 \to J/\psi K^0_S$ mode through the interchange of all d and s quarks (U-spin symmetry, a subgroup of $SU(3)$) [7], leading to a one-to-one correspondence between all decay topologies of these two modes, as illustrated in Fig. 1. Moreover, the $B^0_s \to J/\psi K^0_S$ penguin topologies are not CKM suppressed relative to the tree diagram, as is the case for their B^0 counterparts. A further discussion regarding the theory of this decay and its potential use in LHCb is given in Ref. [8].

To determine the parameters related to the penguin contributions in these decays, a time-dependent CP violation study of the $B^0_s \to J/\psi K^0_S$ mode is required. The determination of its branching fraction, previously measured by CDF [9] and LHCb [10], was an important first step, allowing a test of the U-spin symmetry assumption that lies at the basis of the proposed approach. The second step towards the time-dependent CP violation study is the measurement of the effective $B^0_s \to J/\psi K^0_S$ lifetime, formally defined as [11]

$$\tau^{\text{eff}}_{J/\psi K^0_S} \equiv \frac{\int_0^\infty t \langle \Gamma(B_s(t) \to J/\psi K^0_S)\rangle \, \mathrm{d}t}{\int_0^\infty \langle \Gamma(B_s(t) \to J/\psi K^0_S)\rangle \, \mathrm{d}t}, \tag{1}$$

where

$$\left\langle \Gamma\left(B_s(t) \to J/\psi K^0_S\right)\right\rangle = \Gamma\left(B^0_s(t) \to J/\psi K^0_S\right) + \Gamma\left(\overline{B}^0_s(t) \to J/\psi K^0_S\right) \tag{2}$$

$$= R_{\mathrm{H}} e^{-\Gamma_{\mathrm{H}} t} + R_{\mathrm{L}} e^{-\Gamma_{\mathrm{L}} t} \tag{3}$$

is the untagged decay time distribution, under the assumption that CP violation in B^0_s–$\overline{B}^0_s$ mixing can be neglected [6]. Due to the non-zero decay width difference $\Delta\Gamma_s \equiv \Gamma_{\mathrm{H}} - \Gamma_{\mathrm{L}} = 0.106 \pm 0.013\ \mathrm{ps}^{-1}$ [12] between the heavy and light B^0_s mass eigenstates, the effective lifetime does not coincide with the B^0_s lifetime $\tau_{B^0_s} \equiv 1/\Gamma_s = 1.513 \pm 0.011$ ps [12], where $\Gamma_s = (\Gamma_{\mathrm{H}} + \Gamma_{\mathrm{L}})/2$ is the average B^0_s decay width. Instead, it depends on the decay mode specific relative contributions R_{H} and R_{L}. These two parameters also define the CP observable

$$\mathcal{A}_{\Delta\Gamma_s} \equiv \frac{R_{\mathrm{H}} - R_{\mathrm{L}}}{R_{\mathrm{H}} + R_{\mathrm{L}}}, \tag{4}$$

which allows the effective lifetime to be expressed as [11]

$$\tau^{\text{eff}}_{J/\psi K^0_S} = \frac{\tau_{B^0_s}}{1-y_s^2}\frac{1+2\mathcal{A}_{\Delta\Gamma_s}y_s+y_s^2}{1+\mathcal{A}_{\Delta\Gamma_s}y_s}, \tag{5}$$

where $y_s \equiv \Delta\Gamma_s/2\Gamma_s$ is the normalised decay width difference. For the $B^0_s \to J/\psi K^0_S$ mode, the value of $\mathcal{A}_{\Delta\Gamma_s}$ depends on the penguin contributions, and in particular on their relative weak phase ϕ_s [7]. Using the latest estimates on the size of the $B^0_s \to J/\psi K^0_S$ penguin contributions [13] gives $\mathcal{A}_{\Delta\Gamma_s} = 0.944 \pm 0.066$ and the SM prediction

$$\tau^{\text{eff}}_{J/\psi K^0_S}\big|_{\text{SM}} = 1.639 \pm 0.022 \text{ ps}. \tag{6}$$

Effective lifetime measurements have been performed for the $B^0_s \to K^+K^-$ [14] and $B^0_s \to J/\psi f_0(980)$ [15] decay modes.

This paper presents the first measurement of the effective $B^0_s \to J/\psi K^0_S$ lifetime, as well as an update of the time-integrated branching fraction measurement in Ref. [10], performed with a data sample, corresponding to an integrated luminosity of 1.0 fb^{-1} of pp collisions, recorded at a centre-of-mass energy of 7 TeV by the LHCb experiment in 2011.

The LHCb detector [16] is a single-arm forward spectrometer covering the pseudorapidity range $2 < \eta < 5$, designed for the study of particles containing b or c quarks. The detector includes a high precision tracking system consisting of a silicon-strip vertex detector surrounding the pp interaction region, a large-area silicon-strip detector located upstream of a dipole magnet with a bending power of about 4 Tm, and three stations of silicon-strip detectors and straw drift tubes placed downstream. The combined tracking system has momentum resolution $\Delta p/p$ that varies from 0.4% at 5 GeV/c to 0.6% at 100 GeV/c, and impact parameter resolution of 20 μm for tracks with high transverse momentum (p_{T}) with respect to the beam direction. Charged hadrons are identified using two ring-imaging Cherenkov detectors [17]. Photon, electron and hadron candidates are identified by a calorimeter system consisting of scintillating-pad and preshower detectors, an electromagnetic calorimeter and a hadronic calorimeter. Muons are identified by a system composed of alternating layers of iron and multiwire proportional chambers.

Events are selected by a trigger system [18] consisting of a hardware trigger, which requires muon or hadron candidates with high p_{T}, followed by a two-stage software trigger. In the first stage a partial event reconstruction is performed. For this analysis, events are required to have either two oppositely charged muons with combined mass above 2.7 GeV/c^2, or at least one muon or one high-p_{T} track ($p_{\text{T}} > 1.8$ GeV/c) with a large impact parameter with respect to all pp interaction vertices (PVs). In the second stage a full event reconstruction is performed and only events containing $J/\psi \to \mu^+\mu^-$ candidates are retained.

The signal simulation samples used for this analysis are generated using PYTHIA 6.4 [19] with a specific LHCb configuration [20]. Decays of hadronic particles are described by EVTGEN [21] in which final state radiation is generated using PHOTOS [22]. The interaction of the generated particles with the detector and its response are implemented using the GEANT4 toolkit [23] as described in Ref. [24].

2. Data samples and initial selection

Candidate $B \to J/\psi K^0_S$ decays are reconstructed in the $J/\psi \to \mu^+\mu^-$ and $K^0_S \to \pi^+\pi^-$ final state. Candidate $J/\psi \to \mu^+\mu^-$ decays are required to form a good quality vertex and have a mass in the range [3030, 3150] MeV/c^2. This interval corresponds to about eight times the

$\mu^+\mu^-$ mass resolution at the J/ψ mass and covers part of the J/ψ radiative tail. The selected J/ψ candidate is required to satisfy the trigger decision at both software trigger stages. The K^0_S selection requires two oppositely charged particles reconstructed in the tracking stations placed on either side of the magnet, both with hits in the vertex detector ('long K^0_S' candidate) or without ('downstream K^0_S' candidate). The long (downstream) $K^0_S \to \pi^+\pi^-$ candidates are required to form a good quality vertex and have a mass within 35 (64) MeV/c^2 of the known K^0_S mass [25]. Moreover, to remove contamination from $\Lambda \to p\pi^-$ decays, the reconstructed $p\pi^-$ mass of the long (downstream) K^0_S candidates is required to be more than 6 (10) MeV/c^2 away from the known Λ mass [25]. Furthermore, the K^0_S candidates are required to have a flight distance that is at least five times larger than its uncertainty.

Candidate B mesons are selected from combinations of J/ψ and K^0_S candidates with mass $m_{J/\psi K^0_S}$ in the range [5180, 5520] MeV/c^2. The reconstructed mass and decay time are obtained from a kinematic fit [26] that constrains the masses of the $\mu^+\mu^-$ and $\pi^+\pi^-$ pairs to the known J/ψ and K^0_S masses [25], respectively, and constrains the B candidate to originate from the PV. In case the event has multiple PVs, all combinations are considered. The χ^2 of the fit, which has eight degrees of freedom, is required to be less than 72 and the estimated uncertainty on the B mass must not exceed 30 MeV/c^2. Candidates are required to have a decay time larger than 0.2 ps. To remove misreconstructed $B^0 \to J/\psi K^{*0}$ background that survives the requirement on the K^0_S flight distance, the mass of the long $B^0 \to J/\psi K^0_S$ candidates computed under the $J/\psi K^\pm \pi^\mp$ mass hypotheses must not be within 20 MeV/c^2 of the known B^0 mass [25].

3. Multivariate selection

The loose selection described above does not suppress the combinatorial background sufficiently to isolate the small $B^0_s \to J/\psi K^0_S$ signal. The initial selection is therefore followed by a multivariate analysis, based on a neural network (NN) [27]. The NN classifier's output is used as the final selection variable.

The NN is trained entirely on data, using the $B^0 \to J/\psi K^0_S$ signal as a proxy for the $B^0_s \to J/\psi K^0_S$ decay. The training sample is taken from the mass windows [5180, 5340] MeV/c^2 and [5390, 5520] MeV/c^2, thus avoiding the B^0_s signal region. A normalisation sample consisting of one quarter of the candidates, selected at random, is left out of the NN training to allow an unbiased measurement of the B^0 yield. The signal and background weights are determined using the *sPlot* technique [28] and obtained by performing an unbinned maximum likelihood fit to the mass distribution of the candidates surviving the loose selection criteria. The fitted probability density function (PDF) is defined as the sum of a B^0 signal component and a combinatorial background. The parametrisation of the individual components is described in more detail in the next section.

Due to the differences in the distributions of the input variables of the NN, as well as the different initial signal to background ratio, the multivariate selection is performed separately for the B candidate samples containing long and downstream K^0_S candidates. In the remainder of this paper, these two datasets will be referred to as the long and downstream K^0_S sample, respectively. The NN classifiers use information about the candidate kinematics, vertex and track quality, impact parameter, particle identification information from the RICH and muon detectors, as well as global event properties like track and interaction vertex multiplicities. The variables that are used in the NN are chosen to avoid correlations with the reconstructed B mass.

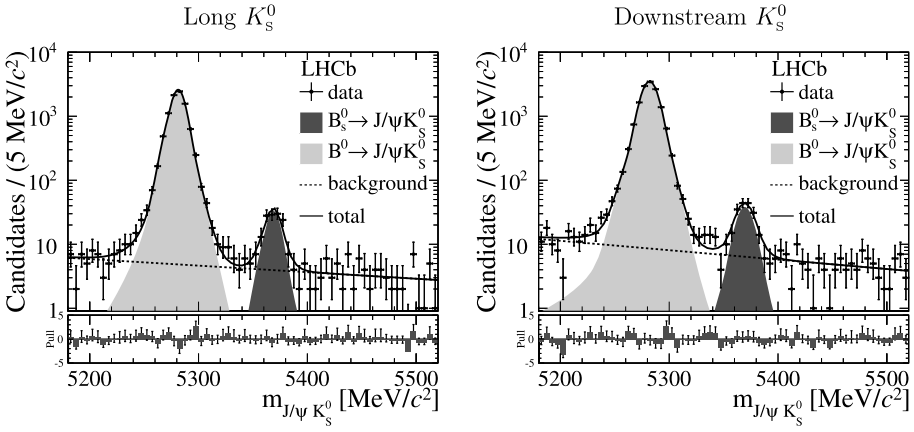

Fig. 2. Fitted $B \to J/\psi K^0_S$ candidate mass distributions and their associated residual uncertainties (pulls) for the (left) long and (right) downstream K^0_S samples, after applying the final requirement on the NN classifier outputs.

Final selection requirements on the NN classifier outputs are chosen to optimise the expected sensitivity to the B^0_s signal observation. The expected signal and background yields entering the calculation of the figure of merit [29] are obtained from the normalisation sample by scaling the number of fitted B^0 candidates, and by counting the number of events in the mass ranges $[5180, 5240]\,\text{MeV}/c^2$ and $[5400, 5520]\,\text{MeV}/c^2$, respectively. After applying the final requirement on the NN classifier output associated with the long (downstream) K^0_S sample, the multivariate selection rejects, relative to the initial selection, 98.7% (99.6%) of the background while keeping 71.5% (50.2%) of the B^0 signal. Due to the worse initial signal to background ratio, the final requirement on the NN classifier output is much tighter in the downstream K^0_S sample than in the long K^0_S sample.

After applying the full selection, the B candidate can still be associated with more than one PV in about 1% of the events. Likewise, about 0.1% of the selected events have several candidates sharing one or more tracks. In these cases, respectively one of the surviving PVs and one of the candidates is used at random.

4. Event yields

For the candidates passing the NN requirements, the ratio of B^0_s and B^0 yields is determined from an unbinned maximum likelihood fit to the mass distribution of the reconstructed B candidates. The fitted PDF is defined as the sum of a B^0 signal component, a B^0_s signal component and a combinatorial background. The B^0_s component is constrained to have the same shape as the B^0 PDF, shifted by the known B^0_s–B^0 mass difference [30]. The mass lineshapes of the $B \to J/\psi K^0_S$ modes in both data and simulation exhibit non-Gaussian tails on both sides of their signal peaks due to final state radiation, the detector resolution and its dependence on the decay angles. Each individual signal shape is parametrised by a double-sided Crystal Ball (CB) function [31]. The parameters describing the CB tails are taken from simulation; all other parameters are allowed to vary in the fit. The background contribution is described by an exponential function.

The results of the fits are shown in Fig. 2, and the fitted yields are listed in Table 1. The B^0 yield is determined in the normalisation sample and scaled to the full sample, whereas the B^0_s

Table 1
Signal yields from the unbinned maximum likelihood fits to the $B \to J/\psi K^0_S$ candidate mass distributions. The uncertainties are statistical only. The yield ratio is calculated from the quantities highlighted in boldface, where the fitted B^0 yield is first multiplied by a factor of four.

Sample	Yield	Long K^0_S	Downstream K^0_S
Normalisation	$\mathbf{B^0 \to J/\psi K^0_S}$	$\mathbf{2205 \pm 47}$	$\mathbf{3651 \pm 61}$
	$B^0_s \to J/\psi K^0_S$	21 ± 5	49 ± 8
	Background	56 ± 11	110 ± 16
Full	$B^0 \to J/\psi K^0_S$	9031 ± 96	$14{,}391 \pm 122$
	$\mathbf{B^0_s \to J/\psi K^0_S}$	$\mathbf{115 \pm 12}$	$\mathbf{158 \pm 15}$
	Background	287 ± 23	490 ± 32
Yield ratio $R \equiv N^{\text{Full}}_{B^0_s \to J/\psi K^0_S} / 4 N^{\text{Norm}}_{B^0 \to J/\psi K^0_S}$		0.0131 ± 0.0014	0.0108 ± 0.0010
Average yield ratio R		0.0116 ± 0.0008	

yield is obtained directly from the full sample. The scaled B^0 yield, obtained from the unbiased sample, differs from the corresponding fit result in the full sample by -211 ± 211 events for the long K^0_S sample and by 213 ± 273 events for the downstream K^0_S sample. Both results are in good agreement, showing that the NN is not overtrained. The yield ratios obtained from the long and downstream K^0_S samples are compatible with each other and are combined using a weighted average.

5. Decay time distribution

Following the procedure explained in Ref. [32], the effective $B^0_s \to J/\psi K^0_S$ lifetime is determined by fitting a single exponential function $g(t) \propto \exp(-t/\tau_{\text{single}})$ to the decay time distribution of the $B^0_s \to J/\psi K^0_S$ signal candidates. In this analysis, the exponential shape parameter τ_{single} is determined from a two-dimensional unbinned maximum likelihood fit to the mass and decay time distribution of the reconstructed B candidates. The fitted PDF is again defined as the sum of a B^0 signal component, a B^0_s signal component and a combinatorial background. The freely varying parameters in the fit are the signal and background yields, and the parameters describing the acceptance, mass and background decay time distributions.

The decay time distribution of each of the two signal components needs to be corrected with a decay time resolution and acceptance model to account for detector effects. The shape of the acceptance function affecting the $B^0_s \to J/\psi K^0_S$ mode is, like the lineshape of its mass distribution, assumed to be identical to that of the $B^0 \to J/\psi K^0_S$ component. The acceptance function is obtained directly from the data using the $B^0 \to J/\psi K^0_S$ mode. Contrary to the B^0_s system, the B^0 system has a negligible decay width difference $\Delta\Gamma_d$ [25]. The decay time distribution of the $B^0 \to J/\psi K^0_S$ channel is therefore fully described by a single exponential function with known lifetime $\tau_{B^0} = 1.519$ ps [6]. Hence, fixing the B^0 lifetime to its known value allows the acceptance parameters to be determined from the fit.

From simulation studies it is found that the decay time acceptance of both signal components is well modelled by the function

$$f_{\text{Acc}}(t) = \frac{1 + \beta t}{1 + (\lambda t)^{-\kappa}}. \tag{7}$$

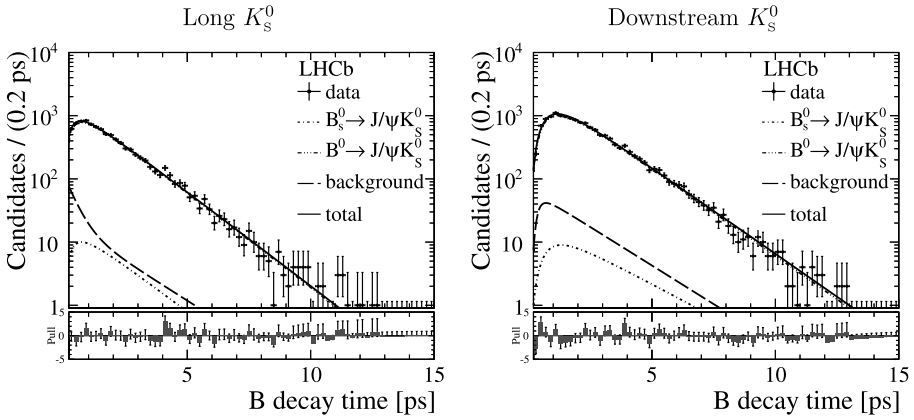

Fig. 3. Fitted $B \to J/\psi K^0_S$ candidate decay time distributions and their associated residual uncertainties (pulls) for the (left) long and (right) downstream K^0_S samples, after applying the final requirement on the NN classifier outputs.

The parameter β describes the fall in the acceptance at large decay times [12]. The parameters κ and λ model the turn-on curve, caused by the use of decay time biasing triggers, the initial selection requirements and, most importantly, the NN classifier outputs.

The decay time resolution for the signal and background components is determined from candidates that have an unphysical, negative decay time. Due to the requirement of 0.2 ps on the decay time of the B candidates applied in the initial selection, such events are not present in the analysed data sample. Instead, a second sample, that is prescaled and does not have the decay time requirement, is used. This sample consists primarily of J/ψ mesons produced at the PV which are combined with a random K^0_S candidate. The decay time distribution for these events is a good measure of the decay time resolution and is modelled by the sum of three Gaussian functions sharing a common mean. Two of the Gaussian functions parametrise the inner core of the resolution function, while the third describes the small fraction of outliers.

The background decay time distributions are studied directly using the data. Their shape is obtained from background candidates that are isolated using the background weights determined by the *sPlot* technique, and cross-checked using the high mass sideband. The exact values of the shape parameters are determined in the nominal fit. Because of the differences induced by the multivariate selection, the background decay time distribution of the long and downstream K^0_S samples cannot be parametrised using the same background model. For the long K^0_S sample, the background is modelled by two exponential functions, describing a short-lived and a long-lived component, respectively. In the downstream K^0_S sample such a short-lived component is not present due to the tighter requirement on the NN classifier output. Its decay time distribution is better described by a single exponential shape corrected by the acceptance function in Eq. (7) with independent parameters $(\kappa', \alpha', \beta')$. The parameter β' is set to zero because we also fit the lifetime of the single exponential function itself, and the combination of both parameters would result in ambiguous solutions.

The decay time distributions resulting from the two-dimensional fits are shown in Figs. 3 and 4 for candidates in the full mass range $m_{J/\psi K^0_S} \in [5180, 5520]\ \mathrm{MeV}/c^2$ and in the B^0_s signal region $m_{J/\psi K^0_S} \in [5340, 5390]\ \mathrm{MeV}/c^2$, respectively. The fitted values are $\tau_{\mathrm{single}} = 1.54 \pm 0.17$ ps and $\tau_{\mathrm{single}} = 1.96 \pm 0.17$ ps for the long and downstream K^0_S sample, respectively. The 1.7σ

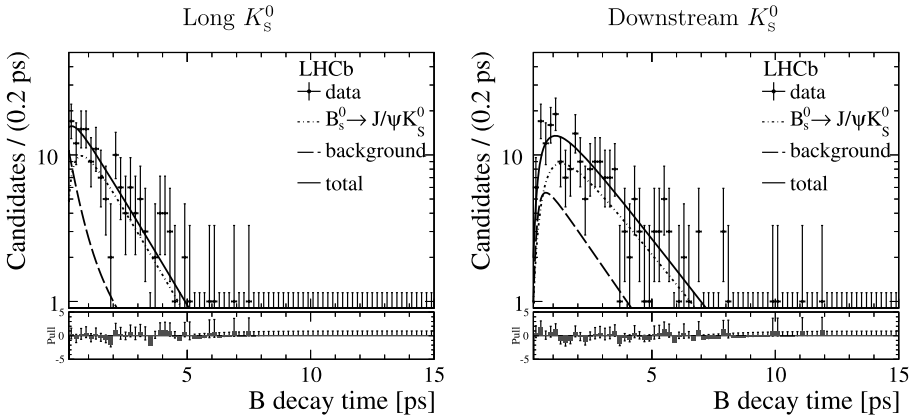

Fig. 4. Fitted $B \to J/\psi K^0_S$ candidate decay time distributions and their associated residual uncertainties (pulls) for the (left) long and (right) downstream K^0_S candidates in the B^0_s signal region $m_{J/\psi K^0_S} \in [5340, 5390]$ MeV/c^2, after applying the final requirement on the NN classifier outputs.

difference between both results is understood as a statistical fluctuation. The two main fit results are therefore combined using a weighted average, leading to

$$\tau_{\text{single}} = 1.75 \pm 0.12 \text{ ps},$$

where the uncertainty is statistical only. The event yields obtained from the two-dimensional fits are compatible with the results quoted in Table 1.

6. Corrections and systematic uncertainties

A number of systematic uncertainties affecting the relative branching fraction $\mathcal{B}(B^0_s \to J/\psi K^0_S)/\mathcal{B}(B^0 \to J/\psi K^0_S)$ and the effective lifetime are considered. The sources affecting the ratio of branching fractions are discussed first, followed by those contributing to the effective lifetime measurement.

The largest systematic uncertainty on the yield ratio comes from the mass shape model, and in particular from the uncertainty on the fraction of the $B^0 \to J/\psi K^0_S$ component's high mass tail extending below the B^0_s signal. The magnitude of this effect is studied by allowing both tails of the CB shapes to vary in the fit. The largest observed deviation in the yield ratios is 3.4%, which is taken as a systematic uncertainty. The mass resolution, and hence the widths of the CB shapes, is assumed to be identical for the B^0 and B^0_s signal modes, but could in principle depend on the mass of the reconstructed B candidate. This effect is studied by multiplying the CB widths of the B^0_s signal PDF by different scale factors, obtained by comparing B^0 and B^0_s signal shapes in simulation. The largest observed difference in the yield ratios is 1.4%, which is taken as a systematic uncertainty. Varying the B^0_s–B^0 mass difference within its uncertainty has negligible effect on the yield ratios.

The selection procedure is designed to be independent of the reconstructed B mass. Simulated data is used to check this assumption, and to evaluate the difference in selection efficiency arising from the different shapes of the $B^0 \to J/\psi K^0_S$ and $B^0_s \to J/\psi K^0_S$ decay time distributions. The ratio of total selection efficiencies is equal to 0.968 ± 0.007, and is used to correct the yield ratio.

Table 2
Corrections and systematic uncertainties on the yield ratio.

Source	Value
Fit model	1.000 ± 0.034
B_s^0 mass resolution	1.000 ± 0.014
Selection efficiency	0.968 ± 0.007
Total correction $f_{\rm corr}^{\mathcal{B}}$	0.968 ± 0.034

The stability of the multivariate selection is verified by comparing different training schemes and optimisation procedures, as well as by calculating the yield ratios for different subsets of the long and downstream K_S^0 sample. All of these tests give results that are compatible with the measured ratio.

The corrections and systematic uncertainties affecting the branching fraction ratio are listed in Table 2. The total systematic uncertainty is obtained by adding all the uncertainties in quadrature.

The main systematic uncertainties affecting the effective $B_s^0 \to J/\psi K_S^0$ lifetime arise from modelling the different components of the decay time distribution. Their amplitudes are evaluated by comparing the results from the nominal fit to similar fits using alternative parametrisations. All tested fit models give compatible results. The largest observed deviations in $\tau_{\rm single}$ are 3.9% due to modelling of the background decay time distribution, 0.47% due to the acceptance function and 0.39% due to the reconstructed B mass description, all of which are assigned as systematic uncertainties. Variations in the decay time resolution model are found to have negligible impact on $\tau_{\rm single}$.

The assumed value of the B^0 lifetime has a significant impact on the shape of the acceptance function, and the β parameter in particular, which in turn affects the fitted value of $\tau_{\rm single}$. This effect is studied by varying the B^0 lifetime within its uncertainty [25]. The largest observed deviation in $\tau_{\rm single}$ is 0.52%, which is taken as a systematic uncertainty.

The fit method is tested on simulated data using large sets of pseudo-experiments, which have the same mass and decay time distributions as the data. Different datasets are generated using the fitted two-dimensional signal and background distributions, and $\tau_{\rm single}$ is then again fitted to these pseudo-experiments. The fit result is compared with the input value to search for possible biases. From the spread in the fitted values and the accompanying residual distributions, a small bias is found. This bias is attributed to the limited size of the background sample, and the resulting difficulty to constrain the background decay time parameters. A correction factor of 1.002 ± 0.002 is assigned to account for this potential bias.

Due to the presence of a non-trivial acceptance function, the result of fitting a single exponential to the untagged B_s^0 decay time distribution does mathematically not agree with the formal definition of the effective lifetime in Eq. (1), as explained in Ref. [32]. The size and sign of the difference between $\tau_{\rm single}$ and $\tau^{\rm eff}_{J/\psi K_S^0}$ depend on the values of $\tau_{B_s^0}$, y_s, $\mathcal{A}_{\Delta\Gamma_s}$, and the shape of the acceptance function. The difference is calculated with pseudo-experiments that sample the acceptance parameters, $\tau_{B_s^0}$ and y_s from Gaussian distributions related to their respective fitted and known values. Since $\mathcal{A}_{\Delta\Gamma_s}$ is currently not constrained by experiment, it is sampled uniformly from the interval $[-1, 1]$. The average difference between $\tau^{\rm eff}_{J/\psi K_S^0}$ and $\tau_{\rm single}$, obtained using

Table 3
Corrections and systematic uncertainties on the effective $B_s^0 \to J/\psi K_S^0$ lifetime.

Source	Value
Background model	1.000 ± 0.039
Acceptance model	1.000 ± 0.005
Mass model	1.000 ± 0.004
B^0 lifetime	1.000 ± 0.005
Fit method	1.002 ± 0.002
Effective lifetime definition	0.999 ± 0.001
Total correction $f_{\rm corr}^{\rm eff}$	1.001 ± 0.040

the acceptance function affecting the long (downstream) K_S^0 sample, is found to be -0.001 ps (-0.003 ps). A correction factor of 0.999 ± 0.001 is assigned to account for this bias.

The presence of a production asymmetry between the B_s^0 and $\overline{B}_s^0$ mesons could potentially alter the measured value of the effective lifetime, but even for large estimates of the size of this asymmetry, the effect is found to be negligible.

Finally, the systematic uncertainties in the momentum and the decay length scale propagate to the effective lifetime. The size of the former contribution is evaluated by recomputing the decay time while varying the momenta of the final state particles within their uncertainty. The systematic uncertainty due to the decay length scale mainly comes from the track-based alignment. Both effects are found to be negligible.

The stability of the fit is verified by comparing the nominal results with those obtained using different fit ranges, or using only subsets of the long and downstream K_S^0 samples. All these tests give compatible results.

The corrections and systematic uncertainties affecting the effective $B_s^0 \to J/\psi K_S^0$ lifetime are listed in Table 3. The total systematic uncertainty is obtained by adding all the uncertainties in quadrature.

7. Results and conclusion

Using the measured ratio $R = 0.0116 \pm 0.0008$ of $B_s^0 \to J/\psi K_S^0$ and $B^0 \to J/\psi K_S^0$ yields, the correction factor $f_{\rm corr}^{\mathcal{B}} = 0.968 \pm 0.034$, and the ratio of hadronisation fractions $f_s/f_d = 0.256 \pm 0.020$ [33], the ratio of branching fractions is computed to be

$$\begin{aligned}\frac{\mathcal{B}(B_s^0 \to J/\psi K_S^0)}{\mathcal{B}(B^0 \to J/\psi K_S^0)} &= R \times f_{\rm corr}^{\mathcal{B}} \times \frac{f_d}{f_s} \\ &= 0.0439 \pm 0.0032\ (\text{stat}) \pm 0.0015\ (\text{syst}) \pm 0.0034\ (f_s/f_d),\end{aligned}$$

where the quoted uncertainties are statistical, systematic, and due to the uncertainty in f_s/f_d, respectively.

Using the known $B^0 \to J/\psi K^0$ branching fraction [25], the ratio of branching fractions can be converted into a measurement of the time-integrated $B_s^0 \to J/\psi K_S^0$ branching fraction. Taking into account the different rates of B^+B^- and $B^0\overline{B}^0$ pair production at the $\Upsilon(4S)$ resonance $\Gamma(B^+B^-)/\Gamma(B^0\overline{B}^0) = 1.055 \pm 0.025$ [25], the above result is multiplied by the corrected value $\mathcal{B}(B^0 \to J/\psi K^0) = (8.98 \pm 0.35) \times 10^{-4}$ and gives

$$\mathcal{B}\big(B_s^0 \to J/\psi K_S^0\big) = \big[1.97 \pm 0.14\ (\text{stat}) \pm 0.07\ (\text{syst}) \pm 0.15\ (f_s/f_d) \pm 0.08\ \big(\mathcal{B}\big(B^0 \to J/\psi K^0\big)\big)\big] \times 10^{-5},$$

where the last uncertainty comes from the $B^0 \to J/\psi K^0$ branching fraction. This result is compatible with, and more precise than, previous measurements [9,10], and supersedes the previous LHCb measurement. The branching fraction is consistent with expectations from U-spin symmetry [10].

Using $\tau_{\text{single}} = 1.75 \pm 0.12$ ps and the correction factor $f_{\text{corr}}^{\text{eff}} = 1.001 \pm 0.040$, the effective $B_s^0 \to J/\psi K_S^0$ lifetime is given by

$$\begin{aligned}\tau_{J/\psi K_S^0}^{\text{eff}} &= f_{\text{corr}}^{\text{eff}} \times \tau_{\text{single}} \\ &= 1.75 \pm 0.12\ (\text{stat}) \pm 0.07\ (\text{syst})\ \text{ps}.\end{aligned}$$

This is the first measurement of this quantity. The result is compatible with the SM prediction given in Eq. (6).

Acknowledgements

We express our gratitude to our colleagues in the CERN accelerator departments for the excellent performance of the LHC. We thank the technical and administrative staff at the LHCb institutes. We acknowledge support from CERN and from the national agencies: CAPES, CNPq, FAPERJ and FINEP (Brazil); NSFC (China); CNRS/IN2P3 and Region Auvergne (France); BMBF, DFG, HGF and MPG (Germany); SFI (Ireland); INFN (Italy); FOM and NWO (The Netherlands); SCSR (Poland); ANCS/IFA (Romania); MinES, Rosatom, RFBR and NRC "Kurchatov Institute" (Russia); MinECo, XuntaGal and GENCAT (Spain); SNSF and SER (Switzerland); NAS Ukraine (Ukraine); STFC (United Kingdom); NSF (USA). We also acknowledge the support received from the ERC under FP7. The Tier1 computing centres are supported by IN2P3 (France), KIT and BMBF (Germany), INFN (Italy), NWO and SURF (The Netherlands), PIC (Spain), GridPP (United Kingdom). We are thankful for the computing resources put at our disposal by Yandex LLC (Russia), as well as to the communities behind the multiple open source software packages that we depend on.

Open access

References

[1] M. Kobayashi, T. Maskawa, *CP* violation in the renormalizable theory of weak interaction, Prog. Theor. Phys. 49 (1973) 652;
N. Cabibbo, Unitary symmetry and leptonic decays, Phys. Rev. Lett. 10 (1963) 531.

[2] I.I. Bigi, A. Sanda, Notes on the observability of *CP* violation in B decays, Nucl. Phys. B 193 (1981) 85.

[3] Belle Collaboration, I. Adachi, et al., Precise measurement of the *CP* violation parameter $\sin 2\phi_1$ in $B^0 \to (c\bar{c})K^0$ decays, Phys. Rev. Lett. 108 (2012) 171802, arXiv:1201.4643.

[4] BaBar Collaboration, B. Aubert, et al., Measurement of time-dependent *CP* asymmetry in $B^0 \to c\bar{c}K^{(*)0}$ decays, Phys. Rev. D 79 (2009) 072009, arXiv:0902.1708.

[5] UTfit Collaboration, M. Bona, et al., The 2004 UTfit collaboration report on the status of the unitarity triangle in the standard model, JHEP 0507 (2005) 028, arXiv:hep-ph/0501199, updated results and plots available at: http://www.utfit.org/UTfit/;
CKMfitter Group, J. Charles, et al., *CP* violation and the CKM matrix: assessing the impact of the asymmetric *B* factories, Eur. Phys. J. C 41 (2005) 1, arXiv:hep-ph/0406184, updated results and plots available at: http://ckmfitter.in2p3.fr.

[6] Heavy Flavor Averaging Group, Y. Amhis, et al., Averages of b-hadron, c-hadron, and τ-lepton properties as of early 2012, arXiv:1207.1158, updated results and plots available at: http://www.slac.stanford.edu/xorg/hfag/.

[7] R. Fleischer, Extracting γ from $B_{s(d)} \to J/\psi K_S^0$ and $B_{d(s)} \to D_{d(s)}^{+} D_{d(s)}^{-}$, Eur. Phys. J. C 10 (1999) 299, arXiv:hep-ph/9903455.

[8] K. De Bruyn, R. Fleischer, P. Koppenburg, Extracting γ and penguin topologies through *CP* violation in $B_s^0 \to J/\psi K_S^0$, Eur. Phys. J. C 70 (2010) 1025, arXiv:1010.0089;
K. De Bruyn, R. Fleischer, P. Koppenburg, Extracting γ and penguin parameters from $B_s^0 \to J/\psi K_S^0$, arXiv:1012.0840.

[9] CDF Collaboration, T. Aaltonen, et al., Observation of $B_s^0 \to J/\psi K^*(892)^0$ and $B_s^0 \to J/\psi K_S^0$ decays, Phys. Rev. D 83 (2011) 052012, arXiv:1102.1961.

[10] LHCb Collaboration, R. Aaij, et al., Measurement of the $B_s^0 \to J/\psi K_S^0$ branching fraction, Phys. Lett. B 713 (2012) 172, arXiv:1205.0934.

[11] R. Fleischer, R. Knegjens, In pursuit of new physics with $B_s^0 \to K^+K^-$, Eur. Phys. J. C 71 (2011) 1532, arXiv:1011.1096.

[12] LHCb Collaboration, R. Aaij, et al., Measurement of *CP*-violation and the B_s^0 meson decay width difference with $B_s^0 \to J/\psi K^+K^-$ and $B_s^0 \to J/\psi \pi^+\pi^-$ decays, Phys. Rev. D (2013), submitted for publication, arXiv:1304.2600.

[13] R. Fleischer, Penguin effects in $\phi_{d,s}$ determinations, arXiv:1212.2792.

[14] LHCb Collaboration, R. Aaij, et al., Measurement of the effective $B_s^0 \to K^+K^-$ lifetime using a lifetime unbiased selection, Phys. Lett. B 716 (2012) 393, arXiv:1207.5993.

[15] LHCb Collaboration, R. Aaij, et al., Measurement of the $\overline{B}_s^0$ effective lifetime in the $J/\psi f_0(980)$ final state, Phys. Rev. Lett. 109 (2012) 152002, arXiv:1207.0878.

[16] LHCb Collaboration, A.A. Alves Jr., et al., The LHCb detector at the LHC, JINST 3 (2008) S08005.

[17] M. Adinolfi, et al., Performance of the LHCb RICH detector at the LHC, Eur. Phys. J. C (2013), in press, arXiv:1211.6759.

[18] R. Aaij, et al., The LHCb trigger and its performance in 2011, JINST 8 (2013) P04022, http://dx.doi.org/10.1088/1748-0221/8/04/P04022, arXiv:1211.3055.

[19] T. Sjöstrand, S. Mrenna, P. Skands, PYTHIA 6.4 physics and manual, JHEP 0605 (2006) 026, arXiv:hep-ph/0603175.

[20] I. Belyaev, et al., Handling of the generation of primary events in GAUSS, the LHCb simulation framework, in: Nuclear Science Symposium Conference Record (NSS/MIC), IEEE, 2010, p. 1155.

[21] D.J. Lange, The EVTGEN particle decay simulation package, Nucl. Instrum. Meth. A 462 (2001) 152.

[22] P. Golonka, Z. Was, PHOTOS Monte Carlo: a precision tool for QED corrections in Z and W decays, Eur. Phys. J. C 45 (2006) 97, arXiv:hep-ph/0506026.

[23] GEANT4 Collaboration, J. Allison, et al., GEANT4 developments and applications, IEEE Trans. Nucl. Sci. 53 (2006) 270;
GEANT4 Collaboration, S. Agostinelli, et al., GEANT4: a simulation toolkit, Nucl. Instrum. Meth. A 506 (2003) 250.

[24] M. Clemencic, et al., The LHCb simulation application, GAUSS: design, evolution and experience, J. Phys.: Conf. Ser. 331 (2011) 032023.

[25] Particle Data Group, J. Beringer, et al., Review of particle physics, Phys. Rev. D 86 (2012) 010001.

[26] W.D. Hulsbergen, Decay chain fitting with a Kalman filter, Nucl. Instrum. Meth. A 552 (2005) 566, arXiv:physics/0503191.

[27] M. Feindt, A neural Bayesian estimator for conditional probability densities, arXiv:physics/0402093.

[28] M. Pivk, F.R. Le Diberder, *sPlot*: a statistical tool to unfold data distributions, Nucl. Instrum. Meth. A 555 (2005) 356, arXiv:physics/0402083.

[29] G. Punzi, Sensitivity of searches for new signals and its optimization, arXiv:physics/0308063.

[30] LHCb Collaboration, R. Aaij, et al., Measurement of b-hadron masses, Phys. Lett. B 708 (2012) 241, arXiv:1112.4896.

[31] T. Skwarnicki, A study of the radiative cascade transitions between the Upsilon-prime and Upsilon resonances, PhD thesis, Institute of Nuclear Physics, Krakow, 1986, DESY-F31-86-02.
[32] K. De Bruyn, et al., Branching ratio measurements of B_s decays, Phys. Rev. D 86 (2012) 014027, arXiv:1204.1735.
[33] LHCb Collaboration, R. Aaij, et al., Measurement of the ratio of fragmentation functions f_s/f_d and the dependence on B meson kinematics, JHEP 1304 (2013) 001, arXiv:1301.5286.

LHCb Collaboration

R. Aaij [40], C. Abellan Beteta [35,n], B. Adeva [36], M. Adinolfi [45], C. Adrover [6], A. Affolder [51], Z. Ajaltouni [5], J. Albrecht [9], F. Alessio [37], M. Alexander [50], S. Ali [40], G. Alkhazov [29], P. Alvarez Cartelle [36], A.A. Alves Jr. [24,37], S. Amato [2], S. Amerio [21], Y. Amhis [7], L. Anderlini [17,f], J. Anderson [39], R. Andreassen [56], R.B. Appleby [53], O. Aquines Gutierrez [10], F. Archilli [18], A. Artamonov [34], M. Artuso [57], E. Aslanides [6], G. Auriemma [24,m], S. Bachmann [11], J.J. Back [47], C. Baesso [58], V. Balagura [30], W. Baldini [16], R.J. Barlow [53], C. Barschel [37], S. Barsuk [7], W. Barter [46], Th. Bauer [40], A. Bay [38], J. Beddow [50], F. Bedeschi [22], I. Bediaga [1], S. Belogurov [30], K. Belous [34], I. Belyaev [30], E. Ben-Haim [8], G. Bencivenni [18], S. Benson [49], J. Benton [45], A. Berezhnoy [31], R. Bernet [39], M.-O. Bettler [46], M. van Beuzekom [40], A. Bien [11], S. Bifani [44], T. Bird [53], A. Bizzeti [17,h], P.M. Bjørnstad [53], T. Blake [37], F. Blanc [38], J. Blouw [11], S. Blusk [57], V. Bocci [24], A. Bondar [33], N. Bondar [29], W. Bonivento [15], S. Borghi [53], A. Borgia [57], T.J.V. Bowcock [51], E. Bowen [39], C. Bozzi [16], T. Brambach [9], J. van den Brand [41], J. Bressieux [38], D. Brett [53], M. Britsch [10], T. Britton [57], N.H. Brook [45], H. Brown [51], I. Burducea [28], A. Bursche [39], G. Busetto [21,q], J. Buytaert [37], S. Cadeddu [15], O. Callot [7], M. Calvi [20,j], M. Calvo Gomez [35,n], A. Camboni [35], P. Campana [18,37], D. Campora Perez [37], A. Carbone [14,c], G. Carboni [23,k], R. Cardinale [19,i], A. Cardini [15], H. Carranza-Mejia [49], L. Carson [52], K. Carvalho Akiba [2], G. Casse [51], L. Castillo Garcia [37], M. Cattaneo [37], Ch. Cauet [9], M. Charles [54], Ph. Charpentier [37], P. Chen [3,38], N. Chiapolini [39], M. Chrzaszcz [25], K. Ciba [37], X. Cid Vidal [37], G. Ciezarek [52], P.E.L. Clarke [49], M. Clemencic [37], H.V. Cliff [46], J. Closier [37], C. Coca [28], V. Coco [40], J. Cogan [6], E. Cogneras [5], P. Collins [37], A. Comerma-Montells [35], A. Contu [15,37], A. Cook [45], M. Coombes [45], S. Coquereau [8], G. Corti [37], B. Couturier [37], G.A. Cowan [49], D.C. Craik [47], S. Cunliffe [52], R. Currie [49], C. D'Ambrosio [37], P. David [8], P.N.Y. David [40], A. Davis [56], I. De Bonis [4], K. De Bruyn [40,*], S. De Capua [53], M. De Cian [39], J.M. De Miranda [1], L. De Paula [2], W. De Silva [56], P. De Simone [18], D. Decamp [4], M. Deckenhoff [9], L. Del Buono [8], N. Déléage [4],

D. Derkach [14], O. Deschamps [5], F. Dettori [41], A. Di Canto [11], F. Di Ruscio [23,k], H. Dijkstra [37], M. Dogaru [28], S. Donleavy [51], F. Dordei [11], A. Dosil Suárez [36], D. Dossett [47], A. Dovbnya [42], F. Dupertuis [38], R. Dzhelyadin [34], A. Dziurda [25], A. Dzyuba [29], S. Easo [48,37], U. Egede [52], V. Egorychev [30], S. Eidelman [33], D. van Eijk [40], S. Eisenhardt [49], U. Eitschberger [9], R. Ekelhof [9], L. Eklund [50,37], I. El Rifai [5], Ch. Elsasser [39], D. Elsby [44], A. Falabella [14,e], C. Färber [11], G. Fardell [49], C. Farinelli [40], S. Farry [12], V. Fave [38], D. Ferguson [49], V. Fernandez Albor [36], F. Ferreira Rodrigues [1], M. Ferro-Luzzi [37], S. Filippov [32], M. Fiore [16], C. Fitzpatrick [37], M. Fontana [10], F. Fontanelli [19,i], R. Forty [37], O. Francisco [2], M. Frank [37], C. Frei [37], M. Frosini [17,f], S. Furcas [20], E. Furfaro [23,k], A. Gallas Torreira [36], D. Galli [14,c], M. Gandelman [2], P. Gandini [57], Y. Gao [3], J. Garofoli [57], P. Garosi [53], J. Garra Tico [46], L. Garrido [35], C. Gaspar [37], R. Gauld [54], E. Gersabeck [11], M. Gersabeck [53], T. Gershon [47,37], Ph. Ghez [4], V. Gibson [46], V.V. Gligorov [37], C. Göbel [58], D. Golubkov [30], A. Golutvin [52,30,37], A. Gomes [2], H. Gordon [54], M. Grabalosa Gándara [5], R. Graciani Diaz [35], L.A. Granado Cardoso [37], E. Graugés [35], G. Graziani [17], A. Grecu [28], E. Greening [54], S. Gregson [46], P. Griffith [44], O. Grünberg [59], B. Gui [57], E. Gushchin [32], Yu. Guz [34,37], T. Gys [37], C. Hadjivasiliou [57], G. Haefeli [38], C. Haen [37], S.C. Haines [46], S. Hall [52], T. Hampson [45], S. Hansmann-Menzemer [11], N. Harnew [54], S.T. Harnew [45], J. Harrison [53], T. Hartmann [59], J. He [37], V. Heijne [40], K. Hennessy [51], P. Henrard [5], J.A. Hernando Morata [36], E. van Herwijnen [37], E. Hicks [51], D. Hill [54], M. Hoballah [5], C. Hombach [53], P. Hopchev [4], W. Hulsbergen [40], P. Hunt [54], T. Huse [51], N. Hussain [54], D. Hutchcroft [51], D. Hynds [50], V. Iakovenko [43], M. Idzik [26], P. Ilten [12], R. Jacobsson [37], A. Jaeger [11], E. Jans [40], P. Jaton [38], F. Jing [3], M. John [54], D. Johnson [54], C.R. Jones [46], C. Joram [37], B. Jost [37], M. Kaballo [9], S. Kandybei [42], M. Karacson [37], T.M. Karbach [37], I.R. Kenyon [44], U. Kerzel [37], T. Ketel [41], A. Keune [38], B. Khanji [20], O. Kochebina [7], I. Komarov [38], R.F. Koopman [41], P. Koppenburg [40], M. Korolev [31], A. Kozlinskiy [40], L. Kravchuk [32], K. Kreplin [11], M. Kreps [47], G. Krocker [11], P. Krokovny [33], F. Kruse [9], M. Kucharczyk [20,25,j], V. Kudryavtsev [33], T. Kvaratskheliya [30,37], V.N. La Thi [38], D. Lacarrere [37], G. Lafferty [53], A. Lai [15], D. Lambert [49], R.W. Lambert [41], E. Lanciotti [37], G. Lanfranchi [18], C. Langenbruch [37], T. Latham [47], C. Lazzeroni [44], R. Le Gac [6], J. van Leerdam [40], J.-P. Lees [4],

R. Lefèvre [5], A. Leflat [31], J. Lefrançois [7], S. Leo [22], O. Leroy [6], T. Lesiak [25], B. Leverington [11], Y. Li [3], L. Li Gioi [5], M. Liles [51], R. Lindner [37], C. Linn [11], B. Liu [3], G. Liu [37], S. Lohn [37], I. Longstaff [50], J.H. Lopes [2], E. Lopez Asamar [35], N. Lopez-March [38], H. Lu [3], D. Lucchesi [21,q], J. Luisier [38], H. Luo [49], F. Machefert [7], I.V. Machikhiliyan [4,30], F. Maciuc [28], O. Maev [29,37], S. Malde [54], G. Manca [15,d], G. Mancinelli [6], U. Marconi [14], R. Märki [38], J. Marks [11], G. Martellotti [24], A. Martens [8], L. Martin [54], A. Martín Sánchez [7], M. Martinelli [40], D. Martinez Santos [41], D. Martins Tostes [2], A. Massafferri [1], R. Matev [37], Z. Mathe [37], C. Matteuzzi [20], E. Maurice [6], A. Mazurov [16,32,37,e], J. McCarthy [44], A. McNab [53], R. McNulty [12], B. Meadows [56,54], F. Meier [9], M. Meissner [11], M. Merk [40], D.A. Milanes [8], M.-N. Minard [4], J. Molina Rodriguez [58], S. Monteil [5], D. Moran [53], P. Morawski [25], M.J. Morello [22,s], R. Mountain [57], I. Mous [40], F. Muheim [49], K. Müller [39], R. Muresan [28], B. Muryn [26], B. Muster [38], P. Naik [45], T. Nakada [38], R. Nandakumar [48], I. Nasteva [1], M. Needham [49], N. Neufeld [37], A.D. Nguyen [38], T.D. Nguyen [38], C. Nguyen-Mau [38,p], M. Nicol [7], V. Niess [5], R. Niet [9], N. Nikitin [31], T. Nikodem [11], A. Nomerotski [54], A. Novoselov [34], A. Oblakowska-Mucha [26], V. Obraztsov [34], S. Oggero [40], S. Ogilvy [50], O. Okhrimenko [43], R. Oldeman [15,d], M. Orlandea [28], J.M. Otalora Goicochea [2], P. Owen [52], A. Oyanguren [35,o], B.K. Pal [57], A. Palano [13,b], M. Palutan [18], J. Panman [37], A. Papanestis [48], M. Pappagallo [50], C. Parkes [53], C.J. Parkinson [52], G. Passaleva [17], G.D. Patel [51], M. Patel [52], G.N. Patrick [48], C. Patrignani [19,i], C. Pavel-Nicorescu [28], A. Pazos Alvarez [36], A. Pellegrino [40], G. Penso [24,l], M. Pepe Altarelli [37], S. Perazzini [14,c], D.L. Perego [20,j], E. Perez Trigo [36], A. Pérez-Calero Yzquierdo [35], P. Perret [5], M. Perrin-Terrin [6], G. Pessina [20], K. Petridis [52], A. Petrolini [19,i], A. Phan [57], E. Picatoste Olloqui [35], B. Pietrzyk [4], T. Pilař [47], D. Pinci [24], S. Playfer [49], M. Plo Casasus [36], F. Polci [8], G. Polok [25], A. Poluektov [47,33], E. Polycarpo [2], A. Popov [34], D. Popov [10], B. Popovici [28], C. Potterat [35], A. Powell [54], J. Prisciandaro [38], V. Pugatch [43], A. Puig Navarro [38], G. Punzi [22,r], W. Qian [4], J.H. Rademacker [45], B. Rakotomiaramanana [38], M.S. Rangel [2], I. Raniuk [42], N. Rauschmayr [37], G. Raven [41], S. Redford [54], M.M. Reid [47], A.C. dos Reis [1], S. Ricciardi [48], A. Richards [52], K. Rinnert [51], V. Rives Molina [35], D.A. Roa Romero [5], P. Robbe [7], E. Rodrigues [53], P. Rodriguez Perez [36], S. Roiser [37], V. Romanovsky [34],

A. Romero Vidal [36], J. Rouvinet [38], T. Ruf [37], F. Ruffini [22], H. Ruiz [35], P. Ruiz Valls [35,o], G. Sabatino [24,k], J.J. Saborido Silva [36], N. Sagidova [29], P. Sail [50], B. Saitta [15,d], V. Salustino Guimaraes [2], C. Salzmann [39], B. Sanmartin Sedes [36], M. Sannino [19,i], R. Santacesaria [24], C. Santamarina Rios [36], E. Santovetti [23,k], M. Sapunov [6], A. Sarti [18,l], C. Satriano [24,m], A. Satta [23], M. Savrie [16,e], D. Savrina [30,31], P. Schaack [52], M. Schiller [41], H. Schindler [37], M. Schlupp [9], M. Schmelling [10], B. Schmidt [37], O. Schneider [38], A. Schopper [37], M.-H. Schune [7], R. Schwemmer [37], B. Sciascia [18], A. Sciubba [24], M. Seco [36], A. Semennikov [30], K. Senderowska [26], I. Sepp [52], N. Serra [39], J. Serrano [6], P. Seyfert [11], M. Shapkin [34], I. Shapoval [16,42], P. Shatalov [30], Y. Shcheglov [29], T. Shears [51,37], L. Shekhtman [33], O. Shevchenko [42], V. Shevchenko [30], A. Shires [52], R. Silva Coutinho [47], T. Skwarnicki [57], N.A. Smith [51], E. Smith [54,48], M. Smith [53], M.D. Sokoloff [56], F.J.P. Soler [50], F. Soomro [18], D. Souza [45], B. Souza De Paula [2], B. Spaan [9], A. Sparkes [49], P. Spradlin [50], F. Stagni [37], S. Stahl [11], O. Steinkamp [39], S. Stoica [28], S. Stone [57], B. Storaci [39], M. Straticiuc [28], U. Straumann [39], V.K. Subbiah [37], L. Sun [56], S. Swientek [9], V. Syropoulos [41], M. Szczekowski [27], P. Szczypka [38,37], T. Szumlak [26], S. T'Jampens [4], M. Teklishyn [7], E. Teodorescu [28], F. Teubert [37], C. Thomas [54], E. Thomas [37], J. van Tilburg [11], V. Tisserand [4], M. Tobin [38], S. Tolk [41], D. Tonelli [37], S. Topp-Joergensen [54], N. Torr [54], E. Tournefier [4,52], S. Tourneur [38], M.T. Tran [38], M. Tresch [39], A. Tsaregorodtsev [6], P. Tsopelas [40], N. Tuning [40], M. Ubeda Garcia [37], A. Ukleja [27], D. Urner [53], U. Uwer [11], V. Vagnoni [14], G. Valenti [14], R. Vazquez Gomez [35], P. Vazquez Regueiro [36], S. Vecchi [16], J.J. Velthuis [45], M. Veltri [17,g], G. Veneziano [38], M. Vesterinen [37], B. Viaud [7], D. Vieira [2], X. Vilasis-Cardona [35,n], A. Vollhardt [39], D. Volyanskyy [10], D. Voong [45], A. Vorobyev [29], V. Vorobyev [33], C. Voß [59], H. Voss [10], R. Waldi [59], R. Wallace [12], S. Wandernoth [11], J. Wang [57], D.R. Ward [46], N.K. Watson [44], A.D. Webber [53], D. Websdale [52], M. Whitehead [47], J. Wicht [37], J. Wiechczynski [25], D. Wiedner [11], L. Wiggers [40], G. Wilkinson [54], M.P. Williams [47,48], M. Williams [55], F.F. Wilson [48], J. Wishahi [9], M. Witek [25], S.A. Wotton [46], S. Wright [46], S. Wu [3], K. Wyllie [37], Y. Xie [49,37], F. Xing [54], Z. Xing [57], Z. Yang [3], R. Young [49], X. Yuan [3], O. Yushchenko [34], M. Zangoli [14], M. Zavertyaev [10,a], F. Zhang [3], L. Zhang [57], W.C. Zhang [12], Y. Zhang [3], A. Zhelezov [11], A. Zhokhov [30], L. Zhong [3], A. Zvyagin [37]

[1] *Centro Brasileiro de Pesquisas Físicas (CBPF), Rio de Janeiro, Brazil*
[2] *Universidade Federal do Rio de Janeiro (UFRJ), Rio de Janeiro, Brazil*
[3] *Center for High Energy Physics, Tsinghua University, Beijing, China*
[4] *LAPP, Université de Savoie, CNRS/IN2P3, Annecy-Le-Vieux, France*
[5] *Clermont Université, Université Blaise Pascal, CNRS/IN2P3, LPC, Clermont-Ferrand, France*
[6] *CPPM, Aix-Marseille Université, CNRS/IN2P3, Marseille, France*
[7] *LAL, Université Paris-Sud, CNRS/IN2P3, Orsay, France*
[8] *LPNHE, Université Pierre et Marie Curie, Université Paris Diderot, CNRS/IN2P3, Paris, France*
[9] *Fakultät Physik, Technische Universität Dortmund, Dortmund, Germany*
[10] *Max-Planck-Institut für Kernphysik (MPIK), Heidelberg, Germany*
[11] *Physikalisches Institut, Ruprecht-Karls-Universität Heidelberg, Heidelberg, Germany*
[12] *School of Physics, University College Dublin, Dublin, Ireland*
[13] *Sezione INFN di Bari, Bari, Italy*
[14] *Sezione INFN di Bologna, Bologna, Italy*
[15] *Sezione INFN di Cagliari, Cagliari, Italy*
[16] *Sezione INFN di Ferrara, Ferrara, Italy*
[17] *Sezione INFN di Firenze, Firenze, Italy*
[18] *Laboratori Nazionali dell'INFN di Frascati, Frascati, Italy*
[19] *Sezione INFN di Genova, Genova, Italy*
[20] *Sezione INFN di Milano Bicocca, Milano, Italy*
[21] *Sezione INFN di Padova, Padova, Italy*
[22] *Sezione INFN di Pisa, Pisa, Italy*
[23] *Sezione INFN di Roma Tor Vergata, Roma, Italy*
[24] *Sezione INFN di Roma La Sapienza, Roma, Italy*
[25] *Henryk Niewodniczanski Institute of Nuclear Physics Polish Academy of Sciences, Kraków, Poland*
[26] *AGH – University of Science and Technology, Faculty of Physics and Applied Computer Science, Kraków, Poland*
[27] *National Center for Nuclear Research (NCBJ), Warsaw, Poland*
[28] *Horia Hulubei National Institute of Physics and Nuclear Engineering, Bucharest-Magurele, Romania*
[29] *Petersburg Nuclear Physics Institute (PNPI), Gatchina, Russia*
[30] *Institute of Theoretical and Experimental Physics (ITEP), Moscow, Russia*
[31] *Institute of Nuclear Physics, Moscow State University (SINP MSU), Moscow, Russia*
[32] *Institute for Nuclear Research of the Russian Academy of Sciences (INR RAN), Moscow, Russia*
[33] *Budker Institute of Nuclear Physics (SB RAS) and Novosibirsk State University, Novosibirsk, Russia*
[34] *Institute for High Energy Physics (IHEP), Protvino, Russia*
[35] *Universitat de Barcelona, Barcelona, Spain*
[36] *Universidad de Santiago de Compostela, Santiago de Compostela, Spain*
[37] *European Organization for Nuclear Research (CERN), Geneva, Switzerland*
[38] *Ecole Polytechnique Fédérale de Lausanne (EPFL), Lausanne, Switzerland*
[39] *Physik-Institut, Universität Zürich, Zürich, Switzerland*
[40] *Nikhef National Institute for Subatomic Physics, Amsterdam, The Netherlands*
[41] *Nikhef National Institute for Subatomic Physics and VU University Amsterdam, Amsterdam, The Netherlands*
[42] *NSC Kharkiv Institute of Physics and Technology (NSC KIPT), Kharkiv, Ukraine*
[43] *Institute for Nuclear Research of the National Academy of Sciences (KINR), Kyiv, Ukraine*
[44] *University of Birmingham, Birmingham, United Kingdom*
[45] *H.H. Wills Physics Laboratory, University of Bristol, Bristol, United Kingdom*
[46] *Cavendish Laboratory, University of Cambridge, Cambridge, United Kingdom*
[47] *Department of Physics, University of Warwick, Coventry, United Kingdom*
[48] *STFC Rutherford Appleton Laboratory, Didcot, United Kingdom*
[49] *School of Physics and Astronomy, University of Edinburgh, Edinburgh, United Kingdom*
[50] *School of Physics and Astronomy, University of Glasgow, Glasgow, United Kingdom*
[51] *Oliver Lodge Laboratory, University of Liverpool, Liverpool, United Kingdom*
[52] *Imperial College London, London, United Kingdom*
[53] *School of Physics and Astronomy, University of Manchester, Manchester, United Kingdom*
[54] *Department of Physics, University of Oxford, Oxford, United Kingdom*
[55] *Massachusetts Institute of Technology, Cambridge, MA, United States*

[56] *University of Cincinnati, Cincinnati, OH, United States*
[57] *Syracuse University, Syracuse, NY, United States*
[58] *Pontifícia Universidade Católica do Rio de Janeiro (PUC-Rio), Rio de Janeiro, Brazil* [t]
[59] *Institut für Physik, Universität Rostock, Rostock, Germany* [u]

[*] Corresponding author.
E-mail address: debkr@nikhef.nl (K. De Bruyn).
[a] P.N. Lebedev Physical Institute, Russian Academy of Science (LPI RAS), Moscow, Russia.
[b] Università di Bari, Bari, Italy.
[c] Università di Bologna, Bologna, Italy.
[d] Università di Cagliari, Cagliari, Italy.
[e] Università di Ferrara, Ferrara, Italy.
[f] Università di Firenze, Firenze, Italy.
[g] Università di Urbino, Urbino, Italy.
[h] Università di Modena e Reggio Emilia, Modena, Italy.
[i] Università di Genova, Genova, Italy.
[j] Università di Milano Bicocca, Milano, Italy.
[k] Università di Roma Tor Vergata, Roma, Italy.
[l] Università di Roma La Sapienza, Roma, Italy.
[m] Università della Basilicata, Potenza, Italy.
[n] LIFAELS, La Salle, Universitat Ramon Llull, Barcelona, Spain.
[o] IFIC, Universitat de Valencia-CSIC, Valencia, Spain.
[p] Hanoi University of Science, Hanoi, Viet Nam.
[q] Università di Padova, Padova, Italy.
[r] Università di Pisa, Pisa, Italy.
[s] Scuola Normale Superiore, Pisa, Italy.
[t] Associated to: Universidade Federal do Rio de Janeiro (UFRJ), Rio de Janeiro, Brazil.
[u] Associated to: Physikalisches Institut, Ruprecht-Karls-Universität Heidelberg, Heidelberg, Germany.